The variational method and the stochastic-Liouville equation. II. ESR spectral simulation via finite elements[a)]

Arthur E. Stillman,[b)] Gary P. Zientara, and Jack H. Freed

Department of Chemistry, Cornell University, Ithaca, New York 14853

(Received 26 February 1979; accepted 2 April 1979)

A Galerkin finite element (FE) method, closely related to the variational FE method of Zientara and Freed, is developed for the solution of the stochastic Liouville equation (SLE). The particular illustrative application considered is the ESR spectral simulation of the simple axially symmetric g-tensor problem. Both linear and quadratic interpolating functions are considered. It is found for this simple case that the Galerkin FE is almost, but not quite, as efficient as eigenfunction expansions (EE). However, the potential advantages of the Galerkin FE in more complex problems are discussed.

I. INTRODUCTION

Past numerical solutions of the stochastic-Liouville equation (SLE) have relied mainly upon eigenfunction expansion[1] (EE) or finite-difference[2] (FD) methods. Recently, Zientara and Freed[3] have introduced the use of variational methods for solving the SLE. They have demonstrated the applicability and computational convenience of the variational finite element (FE) method in the calculation of chemically induced dynamic nuclear (and electronic) polarizations [CIDN(E)P]. The advantages of the FE method are due to the retention of the differential form of the operators and the continuous spatial representation of the spin-density matrix elements. In the FE formalism, one can choose a trial solution to the partial differential equation (or in our case the SLE) for each geometric region. This allows one maximum flexibility in the choice of functional forms and elemental spin and diffusion properties.[4]

EE solutions have proved very useful for slow-motional electron spin resonance (ESR) spectral simulations,[1] although simulations for spin probes with numerous spin levels[5,6] or complex ordering potentials[6] present formidable computing problems despite tailored algorithms. Because of their conceptual simplicity, FD methods were also used at an early stage in ESR simulations.[7] However, the undesirable features of the spatial discretization and averaging that takes place in a FD treatment are overcome by the basic FE approach.

We must distinguish which of several schemes we shall apply to generate FE solutions for calculating ESR spectra. The variational method, which involves integrating a functional[3] and minimizing variations in that functional integral, is theoretically the most appealing but is often cumbersome in application.[8] Also, functionals for complicated rotational diffusion are not easily derived.[8] The second scheme is the minimization of weighted residuals (MWR),[3,4,8] where a trial solution is inserted into the governing operator equation which is subsequently weighted by some function; then its integral over the space is equated to zero.[9] Many types of MWR methods exist, each identified by the choice of weighting functions. One popular MWR scheme is the Galerkin[4,8,10] method imposed globally (i.e., over the entire space in question). Zientara and Freed have noted[3] that the global Galerkin approach is just the EE method, albeit formulated from a different viewpoint. This study shall introduce the MWR Galerkin–FE method.[8] It differs from the global-Galerkin method because of the segmentation (with no FD-like averaging) of space into elements. It also retains the advantage of Galerkin methods which can implicitly satisfy a variational principle provided the respective functional exists.[8]

The Galerkin–FE method has a major advantage in its quite simple implementation compared to functional based methods. Thus in this work we extend the general use of finite elements to solutions of the SLE when the use of functionals becomes unwieldy or when the functionals cannot be found.

In this work we will compare the use of the EE, FD, and Galerkin–FE numerical methods in the solution of the SLE applied to a relatively simple ESR example. It is hoped that this will aid in our understanding of the theoretical and computational utility of each method. Since variational and MWR-type FE methods can assume the advantages of both numerical and analytic solutions, they should ultimately prove useful when complicated interactions and/or geometries occur in magnetic resonance studies. In Sec. II, the general formalism of the Galerkin–FE method is discussed and then applied in a solution of the SLE. The simple example chosen is the simulation of an ESR spectrum of an electron-spin $S=\frac{1}{2}$ radical with an axially symmetric g tensor, which is undergoing isotropic Brownian rotational diffusion. Results and computational considerations of this method are then compared in Sec. III to those obtained from the EE and FD methods.

II. THE GALERKIN-FINITE ELEMENT METHOD

A. Outline of the method

We first consider an ordinary differential equation in the spatial variable(s)[11] of the form

$$\mathcal{L}(x)f(x)-c=0\ . \tag{2.1}$$

Here $\mathcal{L}(x)$ is some differential operator, $f(x)$ is the exact solution, and c is a constant. [When the spin aspects of the SLE are imposed we shall obtain a coupled set of

---

[a)] Supported by NSF Grant CHE 77-26996 as well as the NRCC under a grant from NSF and U. S. DOE Contract W-7405-ENG-48.

[b)] NSF Postdoctoral Fellow.

equations of the form of Eq. (2.1), but here we limit our discussion to illustrate the major points.] One chooses a trial solution, $g(x)$ for which the residual (error) is defined as

$$R(x) \equiv \mathcal{L}(x)\, g(x) - c \tag{2.2}$$

and which may be expanded in some convenient finite basis set $\{\Phi_i(x)\}$ as

$$g(x) = \sum_{i=1}^{M} g_i\, \Phi_i(x) \;, \tag{2.3}$$

where the g_i shall be considered unknown coefficients while the $\Phi_i(x)$ satisfy the global boundary conditions. In a Galerkin-type MWR method one first weights the corresponding residual by one of the basis functions, integrates and sets this weighted residual to zero, i.e.,

$$\sum_{j=1}^{M} g_j \int_{\text{all } x} \Phi_i(x)\, \mathcal{L}(x)\, \Phi_j(x)\, dx - c \int_{\text{all } x} \Phi_i(x)\, dx = 0 \quad \text{for all } i \tag{2.4}$$

(Here we have assumed a unit Jacobian, which may be altered if necessary without loss of generality.) Equation (2.4) thus generates an $M \times M$ set of equations,

$$\sum_{j=1}^{M} A_{ij}\, g_j = f_i \quad \text{for all } i = 1 \text{ to } M \;, \tag{2.5a}$$

with

$$f_i = c \int_{\text{all } x} \Phi_i(x)\, dx \;. \tag{2.5b}$$

This completes the global Galerkin formulation. However, in the Galerkin–FE method one segments space and proceeds in a fashion similar to the variational-FE approach.

In the Galerkin–FE formalism one distinguishes between global (i.e., all space) or local (i.e., inside an element) functions and indices. These bookkeeping features, although cumbersome initially, provide one much ease in the actual creation of the final matrix equation.

The notation for the global region now involves replacement of the M unknown g_i's of Eq. (2.3) by M unknown values of the function $g[X(i)]\, 1 \le i \le M$, where the M positions $X(i)$ are called the global nodes in x space. The $X(i)$ are chosen at boundaries between elements and/or at points in the interior of an element. To conform to the usual notation we let $g(i) \equiv g[X(i)]$.

Next, one can discuss the function $g(x)$ in the local sense, i.e., within one element. Zientara and Freed made exclusive use of locally determined quantities.[3] When higher-order local interpolating functions are chosen (as in this study) a combination of both global and local functions is useful. Local functions will carry a superscript, (e.g., $f^{(l)}$). Local nodes will be defined at the same spatial positions as global nodes, but they will carry a local index which varies from 1 to say, 2 (or 3) within *each* consecutive element, corresponding to 2 (or 3) nodes per element. This indexing is exhibited in Fig. 1. The transcription relation linking global to local quantities is illustrated by the use in Eq. (2.4) of the substitution

$$\Phi_i(x) = \sum_{l=1}^{L} \sum_{k=1}^{K} \Phi_k^{(l)}(y)\, \Delta_{ki}^{(l)} \tag{2.6}$$

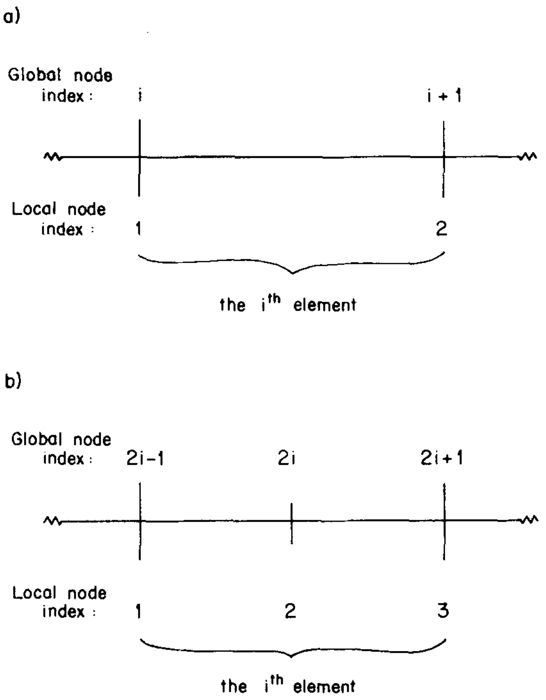

FIG. 1. Global and local nodal indexing for (a) linear interpolating functions with no internal modes, or (b) quadratic interpolating functions with one internal node.

so that

$$g(x) = \sum_{i=1}^{M} \sum_{l=1}^{L} \sum_{k=1}^{K} \Phi_k^{(l)}(y)\, \Delta_{ki}^{(l)}\, g(i) \;, \tag{2.7}$$

where $\Phi_k^{(l)}(y)$ is the kth locally defined interpolation function in the lth element expressed in the local coordinate y defined only in that element. There are K functions $\{\Phi_k^{(l)}\}$ per element and there are L elements. Also,

$$\begin{aligned} \Delta_{ki}^{(l)} = 1 \quad & \text{if the } k\text{th local node} \\ & \text{coincides with the } i\text{th global node} \\ & \text{somewhere in the } l\text{th element,} \\ \Delta_{ki}^{(l)} = 0 \quad & \text{otherwise.} \end{aligned} \tag{2.8}$$

This just "picks out" the correct spatial "pieces" for the piecewise-smooth $\Phi_i(x)$.

What remains is the recalculation of Eq. (2.4) using Eqs. (2.6) and (2.7). The quantities in Eq. (2.5) now become

$$A_{ij} = \sum_{l=1}^{L} \sum_{m,k=1}^{K} \hat{A}_{km}^{(l)}\, \Delta_{ki}^{(l)}\, \Delta_{mj}^{(l)} \tag{2.9}$$

and

$$f_i = \sum_{l=1}^{L} \sum_{k=1}^{K} f_i^{(l)}\, \Delta_{ki}^{(l)} \;, \tag{2.10}$$

so only the equations for a block of dimension $K \times K$ of $\hat{\mathbf{A}}$ need be explicitly written together with the K elements of $\hat{\mathbf{f}}$. These are then added (usually on the computer) by the prescription of Eqs. (2.9) and (2.10). Moreover, when one expresses these matrix or vector elements, the integrations may be shifted to local variables over the elemental "length" rather than over the entire domain of x. The summations in Eqs. (2.9) and (2.10) yield the equations noted by Eq. (2.5), but with the g_j now replaced by the nodal values $g(j)$, and Eq. (2.5) becomes an $N\times N$ set of simultaneous linear equations where $(M\rightarrow N)$:

$$N=(K-1)L+1\ , \tag{2.11}$$

N being the total number of global nodes, K the number of interpolating functions per element [polynomials of order $(K-1)$], and L the total number of elements. Equation (2.5), which usually produces a matrix of banded form, then permits the calculation of the nodal values, $g(j)$, from which the final form of the solution $g(x)$ is constructed from Eq. (2.7).

B. Application to the solution of the SLE

We write the SLE as

$$\frac{\partial\rho(\Omega,t)}{\partial t}=-i\,[\mathcal{H}(\Omega),\ \rho(\Omega,t)]-\Gamma_\Omega\,\rho(\Omega,t)+\mathcal{R}\rho(\Omega,t)\ , \tag{2.12}$$

where $\rho(\Omega,t)$ is the spin density matrix, Ω are the spatial variables (e.g., Euler angles) which are assumed to be stochastic variables, $\mathcal{H}(\Omega)$ is the spin Hamiltonian, Γ_Ω is the stochastic diffusion operator, and $\mathcal{R}$ represents all other contributions to spin relaxation. Upon Fourier transforming Eq. (2.12) and utilizing the appropriate forms of $\mathcal{H}(\Omega)$ and Γ_Ω for the present simulation problem,[1] one obtains for the off-diagonal spin density matrix element, which is related to the absorption,

$$\left[\hat{\mathfrak{a}}(\theta,\omega)+i\,\frac{R}{\sin\theta}\,\frac{\partial}{\partial\theta}\left(\sin\theta\,\frac{\partial}{\partial\theta}\right)\right]Z_\lambda(\theta)-b=0\ , \tag{2.13a}$$

where

$$\hat{\mathfrak{a}}(\theta,\omega)\equiv(\omega-\omega_\lambda)-\tfrac{1}{2}\mathfrak{F}(3\cos^2\theta-1)-iT_2^{-1} \tag{2.13b}$$

and

$$b=d_\lambda\,\omega_\lambda\,q\ . \tag{2.13c}$$

All parameters have been defined elsewhere,[1] so only those pertinent to the present discussion will be noted here: ω is the angular frequency, θ is the angle between the symmetry axis of the radical and the laboratory frame, T_2^{-1} is an orientation independent contribution to the spectral linewidth. $\mathfrak{F}$ is a measure of the asymmetry of the g tensor and R is the rotational diffusion coefficient. $R/|\mathfrak{F}|$ is a convenient measure of the diffusion rate of the radical on the ESR time scale. Thus, $R/|\mathfrak{F}|\gg 1$ represents the motionally narrowed limit. Equation (2.13) must be solved for the unknown function $Z_\lambda(\theta)$. The ESR absorption line shape is then proportional to[1]

$$\begin{aligned}\mathscr{I}(\omega)&=\operatorname{Im}\int_0^\pi d\theta\,\sin\theta\,P_0(\theta)\,Z_\lambda(\theta)\\&=2\operatorname{Im}\int_0^{\pi/2} d\theta\,\sin\theta\,P_0(\theta)\,Z_\lambda(\theta)\ .\end{aligned} \tag{2.14}$$

$P_0(\theta)$ ($=1/2$ for isotropic liquids) is the orientational distribution function at thermal equilibrium.

We shall now apply the general method discussed at the beginning of this section making the proper choices of interpolating functions, element numbers, and element lengths. By the choice of Eq. (2.7) we will attempt to approximate $Z_\lambda(\theta)$ by some trial global solution, $\overline{Z}(\theta)$, having nodal values $\overline{Z}(i)$ for $i=1$ to N, which must be determined. We can treat our problem globally, at first, and write the specific form of Eq. (2.4) [with Eq. (2.1) becoming Eq. (2.13)]:

$$\int_0^\pi d\theta\,\sin\theta\,\Phi_i(\theta)\left\{\left[\hat{\mathfrak{a}}(\theta,\omega)+i\,\frac{R}{\sin\theta}\,\frac{\partial}{\partial\theta}\left(\sin\theta\,\frac{\partial}{\partial\theta}\right)\right]\times\sum_{j=1}^{N}\Phi_j(\theta)\,\overline{Z}(j)-b\right\}=0\ . \tag{2.15}$$

We then integrate the diffusion term of Eq. (2.15) by parts[12] giving the term

$$-iR\int_0^\pi d\theta\,\sin\theta\left(\frac{\partial\Phi_i(\theta)}{\partial\theta}\right)\left(\frac{\partial\Phi_j(\theta)}{\partial\theta}\right)\ .$$

It is conventient at this point to perform the change of variable $x=\cos\theta$ and rewrite Eq. (2.15) (with the simplified integral) as

$$\begin{aligned}&\int_{-1}^{1} dx\,\Phi_i(x)\left\{\left[\omega-\omega_\lambda+\mathfrak{F}/2-\tfrac{3}{2}\mathfrak{F}\left(\sum_k\Phi_k(x)X(k)\right)-iT_2^{-1}\right]\right.\\&\quad\left.\times\sum_{j=1}^{N}\Phi_j(x)\,\overline{Z}(j)-b\right\}-iR\int_{-1}^{1}dx\left[1-\left(\sum_k\Phi_k(x)X(k)\right)^2\right]\\&\quad\times\frac{\partial\Phi_i(x)}{\partial x}\sum_{j=1}^{N}\frac{\partial\Phi_j(x)}{\partial x}\,\overline{Z}(j)=0\ ,\end{aligned} \tag{2.16}$$

where $\overline{Z}(j)$ is now a nodal value of the trial function $\overline{Z}(x)$ and x^2 was replaced with its global nodal value representation, i.e., $X(k)=x$ at the kth global node. Equation (2.16) represents a set of linear simultaneous equations in terms of the unknowns $\overline{Z}(j)$ of the same form as Eq. (2.5). We impose the FE format on our Galerkin scheme by writing our interpolation functions as in Eq. (2.6). Then writing Eq. (2.16) as

$$\sum_j A_{ij}\,\overline{Z}(j)=f_i\ , \tag{2.17}$$

we can complete the first stage of our solution by employing Eqs. (2.9) and (2.10). What remains then is the writing of the several necessary $\mathbf{A}$ and $\hat{\mathbf{f}}$ elements which come from an appropriate choice of local interpolating functions inserted in Eq. (2.6).

We shall obtain $\hat{\mathbf{A}}$ and $\hat{\mathbf{f}}$, or subsequently $\mathbf{A}$ and f for this problem, by using linear local interpolation functions in one example and quadratic functions in another. As mentioned above, for a $(K-1)$th order polynomial interpolation function there will result K local interpolation functions requiring K local nodes. Thus, a linear local approximation $(K=2)$ is associated with[8] these functions in the lth element:

$$\Phi_1^{(l)}(y)=1-y/h^{(l)}\ , \tag{2.18a}$$

$$\Phi_2^{(l)}(y)=y/h^{(l)}\ , \tag{2.18b}$$

where $h^{(l)}$ is the length of the lth element, and all functions follow $0\le\Phi_k^{(l)}\le 1$ setting the limits of the integrations over the local coordinate y. The local coordinate y is related to x by the equation $y=x-X(l)$ in the lth element when a linear approximation is used. One then has

$$\begin{aligned}\hat{A}_{11}^{(l)}&=\mathfrak{a}h^{(l)}/3\\&\quad-\tfrac{3}{2}\mathfrak{F}\,h^{(l)}\,[X(l)^2/5+X(l)X(l+1)/10+X(l+1)^2/30]\\&\quad-\frac{iR}{h^{(l)}}\,[1-\tfrac{1}{3}\{X(l)^2+X(l)X(l+1)+X(l+1)^2\}]\ ,\end{aligned} \tag{2.19a}$$

$$\hat{A}_{12}^{(l)} = \hat{A}_{21}^{(l)}$$
$$= \mathfrak{A} h^{(l)}/6$$
$$- \tfrac{3}{2} \mathfrak{F} h^{(l)} [X(l)^2/20 + X(l)X(l+1)/15 + X(l+1)^2/20]$$
$$+ \frac{iR}{h^{(l)}} [1 - \tfrac{1}{3}\{X(l)^2 + X(l)X(l+1) + X(l+1)^2\}] , \quad (2.19b)$$

$$\hat{A}_{22}^{(l)} = \mathfrak{A} h^{(l)}/3$$
$$- \tfrac{3}{2} \mathfrak{F} h^{(l)} [X(l)^2/30 + X(l)X(l+1)/10 + X(l+1)^2/5]$$
$$- \frac{iR}{h^{(l)}} [1 - \tfrac{1}{3}\{X(l)^2 + X(l)X(l+1) + X(l+1)^2\}] , \quad (2.19c)$$

with

$$\mathfrak{A} \equiv [\omega - \omega_\lambda + \mathfrak{F}/2 - iT_2^{-1}] \quad (2.19d)$$

and

$$\hat{f}_1^{(l)} = \hat{f}_2^{(l)} = bh^{(l)}/2 . \quad (2.20)$$

The transcription relations discussed in Sec. II A readily permit the creation of the **A** matrix. From Eq. (2.9) we have

$$A_{ll} = \hat{A}_{22}^{(l-1)} + \hat{A}_{11}^{(l)} , \quad (2.21a)$$

$$A_{lk} = A_{kl} = \hat{A}_{12}^{(l)} \delta_{l,k+1} , \quad (2.21b)$$

and

$$f_l = \tfrac{1}{2} b (h^{(l-1)} + h^{(l)}) \quad (2.21c)$$

all for $l \neq 1$ or $L+1$ (i.e., not pertaining to the nodes at the edges of the global region) for which we have

$$A_{11} = \hat{A}_{11}^{(1)} , \quad (2.22a)$$

$$A_{L+1,L+1} = \hat{A}_{22}^{(L)} , \quad (2.22b)$$

and

$$f_1 = bh^{(1)}/2 , \quad (2.22c)$$

$$f_{L+1} = bh^{(L)}/2 , \quad (2.22d)$$

noting again from Eq. (2.11) that N (the total number of nodes) $= L+1$ for this linear approximation. Once the matrices are constructed one may solve for the $\overline{Z}(j)$ from $\overline{Z} = \mathbf{A}^{-1}\mathbf{f}$ by standard elimination procedures.

The application of higher order local interpolating functions in the Galerkin–FE solution of the SLE follows in a straightforward manner from the above format. For a quadratic approximation applied within each element ($K=3$) three local nodes will be required. Thus we introduce the use of an interior node. This interior node is usually set at the midpoint of the element. The local interpolation functions then are[8]

$$\Phi_1^{(l)}(y) = \frac{y}{h^{(l)}}\left(\frac{2y}{h^{(l)}} - 1\right) , \quad (2.23a)$$

$$\Phi_2^{(l)}(y) = 1 - (2y/h^{(l)})^2 , \quad (2.23b)$$

and

$$\Phi_3^{(l)}(y) = \frac{y}{h^{(l)}}\left(\frac{2y}{h^{(l)}} + 1\right) , \quad (2.23c)$$

where we have again chosen the functions such that $0 \leq \Phi_k^{(l)} \leq 1$, but now $-h^{(l)}/2 \leq y \leq h^{(l)}/2$ forming the integration limits with $y = x - X(2l)$ in the lth element. One can then generate the equations analogous to Eqs. (2.19), but now the nine matrix elements $\hat{A}_{ij}$ for $i, j = 1$, 2, and 3 must be formulated. It is clear from the form of Eqs. (2.19) that the matrix elements for the quadratic case will contain more terms, yet still involving simple integrals over powers of x. After the nodal values $\overline{Z}(i)$ are computed, one obtains the trial solution to the overall SLE as in Eq. (2.7):

$$\overline{Z}(x) = \sum_{i=1}^{N} \sum_{l=1}^{L} \sum_{k=1}^{K} \Phi_k^{(l)}(y) \Delta_{ki}^{(l)} \overline{Z}(i) , \quad (2.24)$$

and then the spectral line shape is found from Eq. (2.14) which we now rewrite as

$$\mathscr{g}(\omega) = \mathrm{Im}\, \tfrac{1}{2} \int_{-1}^{1} dx \overline{Z}(x) . \quad (2.25)$$

Clearly the use of trial solutions which better approximate the true solution should reduce computational effort. The improvement in the simulated spectral results coming from the quadratic approximation will be discussed below.

While the example given above is really the simplest slow-tumbling case, which we are using for purposes of illustration, the more difficult examples involving the coupling of different spin-density matrix elements can be handled by straightforward generalization of the above approach along the lines we have previously discussed for the CIDN(E)P problem.[3] This fact is important in considering the potential utility of the Galerkin–FE method.

We have also analyzed other MWR methods based on the good results obtained with the Galerkin–FE scheme. In particular, a collocation method[4,8] was also used for the above example. In the collocation method one chooses Dirac delta functions as the weighting functions in an MWR formalism. So, in general, using Eqs. (2.2) and (2.3) we can write

$$\int_{\text{all } x} R(x)\, \delta(x - x_i)\, dx = 0 , \quad (2.26)$$

which we may expand as

$$\sum_{j=1}^{M} g_j [\mathfrak{L}(x) \Phi_j(x)]_{x_i} - c = 0$$
$$\text{for all } i \ (i = 1 \text{ to } I_{\max} \text{ with } I_{\max} \geq M) , \quad (2.27)$$

with $[\mathfrak{L}(x)\Phi_j(x)]_{x_i}$ denoting the result of the operation of $\mathfrak{L}(x)$ on $\Phi_j(x)$ evaluated at x_i. Here one is setting the residual equal to zero only at certain points in space. Although this represents a mathematically less rigorous condition on the trial solution, we have found that the collocation method does reproduce the EE (or FE) results with negligible error. This method is advantageous for complicated problems [i.e., difficult $\mathfrak{L}(x)$ forms] since no integrations are necessary [cf. Eq. (2.27)].

III. COMPARISON OF NUMERICAL APPROACHES

We have found in studying this simple example that, as a general rule (over a wide range of $R/|\mathfrak{F}|$ values) the minimum order of the matrix equation to be solved obeys EE < FE < FD (cf. Table I). Quadratic FE interpolating functions did prove more efficient computationally compared to linear functions in the incipient slow mo-

TABLE I. Minimum order of secular g-tensor matrices.[a]

$R/\lvert\mathfrak{F}\rvert$	EE	$\mathrm{FE}_{1,\theta}$[b]	$\mathrm{FE}_{2,\theta}$[c]	$\mathrm{FE}_{1,x}$[d]	FD_x[e]
0.001[f]	12	16	21	37	80
0.01[f]	6	14	11	18	40
0.1[g]	3	10	7	10	20
1.0[h]	3	10	3	10	20

[a] All calculations were performed with parameters $B_0 = 3300$ G, $g_\parallel = 2.00235$, and $g_\perp = 2.0031$. The calculation was considered to have converged when no further spectral changes were noted upon increasing the number of equations to be solved. By symmetry the FE and FD methods only require $0 \le \theta \le \pi/2$.

[b] Linear FE with an equally spaced grid in θ.

[c] Quadratic FE with an equally spaced grid in θ. Note that the matrix is pentadiagonal in this method.

[d] Linear FE with an equally spaced grid in $x = \cos\theta$.

[e] FD with an equally spaced grid in x.

[f] $T_2^{-1} = 0.01$ G, 2.0 G sweep width.

[g] $T_2^{-1} = 0.005$ G, 1.0 G sweep width.

[h] $T_2^{-1} = 0.005$ G, 0.5 G sweep width.

tional region ($R/\lvert\mathfrak{F}\rvert \lesssim 1$) while the opposite is true for the near rigid limit rotational spectral simulation.

In order to better understand these results, it is instructive to more closely examine the behavior of the solutions obtained by these numerical methods.

A. The eigenfunction expansion and the Galerkin-FE methods

The general EE (or global Galerkin) solution of the secular g-tensor problem is of the form

$$\bar{Z}(x) = \sum_{n=0}^{N} C_{2n} P_{2n}(x) \tag{3.1a}$$

or equivalently

$$\bar{Z}(\theta) = \sum_{n=0}^{N} C_{2n} P_{2n}(\cos\theta) = \sum_{n=0}^{N} D_{2n} \cos(2n\pi\theta) , \tag{3.1b}$$

where $\bar{Z}(x \text{ or } \theta)$ remains an approximate result due to the truncation (at N) of the otherwise infinite expansion. Here the C_k are coefficients of the Legendre polynomial basis and the D_k are the corresponding equivalent Fourier cosine series coefficients. The motionally narrowed limit is well represented by only the $n = 0$ and 1 terms; that is, a quadratic function of x. Thus, we would expect, and indeed have found, a single element in the quadratic Galerkin–FE approximation is sufficient in the motionally narrowed case. To simulate this quadratic solution by continuous linear segments one expects, and finds, that a number of smaller elements are required. Also, as the rotational motion slows and the first two terms of Eq. (3.1) still dominate, one might expect quadratic interpolation functions to be superior.

Near the rigid limit larger values of N in Eq. (3.1) are required for a good spectral fit by EE. Since the $\cos\theta$ and $\cos^2\theta$ functions we have employed in the Galerkin-FE method oscillate relatively slowly, more spatial segmentation (i.e., more elements) is necessary to improve the trial solution. Once many elements are necessary, the quadratic interpolation functions become less convenient than linear functions, because of the greater number of nodes per element in the former case.

B. Finite differences and the Galerkin-FE methods

Some early spectral simulations of slow motional ESR spectra were based upon FD methods.[7] This approach differs from FE in two respects: in FD one assumes the function is constant in the neighborhood of each node.[13] Moreover, in FD continuous diffusion is approximated by finite jumps. This latter feature implies that convergence not only requires enough nodal points that the calculated solution is approximately smooth, but also enough so that continuous diffusion is well represented. Thus, it is to be expected (and Table I confirms) that FE should converge more rapidly than FD methods.

In spite of the greater apparent complexity of the FE formulation of the SLE, the incorporation of boundary conditions is often more straightforward than in FD. This has in fact been found to be the case for our simple secular g-tensor example. Also, FE and FD methods differ in the undesirable feature that the sweep variable appears in the full bandwidth of the FE matrix equations. In EE and FD methods the sweep variable appears only along the diagonal. Best numerical economy may then be achieved by use of diagonalization techniques.[1,7] The FE equations may be rendered approximately diagonal in the sweep variable by performing a FD-like average for the quantum terms. That is, we let

$$\begin{aligned}
&\left[\mathfrak{a} h^{(l-1)}/6 - \tfrac{3}{2}\mathfrak{F} h^{(l-1)}\left(\frac{X(l-1)^2}{20} + \frac{X(l-1)X(l)}{15} + \frac{X(l)^2}{20}\right)\right] Z(l-1)\\
&\quad + \left[\mathfrak{a}(h^{(l-1)} + h^{(l)})/3 - \tfrac{3}{2}\mathfrak{F} h^{(l-1)}\left(\frac{X(l-1)^2}{30} + \frac{X(l-1)X(l)}{10} + \frac{X(l)^2}{5}\right) - \tfrac{3}{2}\mathfrak{F} h^{(l)}\left(\frac{X(l)^2}{5} + \frac{X(l)X(l+1)}{10} + \frac{X(l+1)^2}{30}\right)\right] Z(l)\\
&\quad + \left[\mathfrak{a} h^{(l)}/6 - \tfrac{3}{2}\mathfrak{F} h^{(l)}\left(\frac{X(l)^2}{20} + \frac{X(l)X(l+1)}{15} + \frac{X(l+1)^2}{20}\right)\right] Z(l+1) \approx (\mathfrak{a} - \tfrac{3}{2}\mathfrak{F} X(l)^2)\, h^{(l)} Z(l) ,
\end{aligned} \tag{3.2}$$

where $\mathfrak{a}$ from Eq. (2.19d) includes the sweep variable.[14] As might be expected, this *ad hoc* modification of the FE equation decreases the convergence efficiency. However, one still finds a reduction in the size of the numerical problem compared with that encountered in FD.

IV. CONCLUDING REMARKS

We have considered in this work the simplest of slow-tumbling problems as a basis for and test of FE methods, in particular those based upon the MWR techniques, which are simpler to employ than the variational procedures. These techniques are quite general, so one can readily employ them to cases involving non-Brownian or more complex diffusion as well as to problems involving more complex spin Hamiltonians. In these latter cases one may employ spherical triangular elements to maximize the efficiency of solution.[15] It is our belief that FE methods could prove a useful alternative to EE methods in some of the more complex slow-tumbling problems. Thus, for example, in problems in which there are ordering potentials with complex functional dependences (or alternatively when they are only known numerically) then EE methods become less efficient, while FE methods are relatively unaffected.[16] Such complex potentials may be needed to deal realistically with ordered phases of physical or biological interest.[17]

There is another class of possible applications, which depends upon the continuous nature of the functional representations in FE vs the discontinuous forms of FD. These include the study of the simplication of cases involving more complex spin Hamiltonians (e.g., nitroxides or vanadyl) which can be expressed in diagonal form as a function of orientation, but are in nondiagonal form in terms of EE. The extent to which nonadiabatic transitions, in which a nuclear spin flips (when referred to its local axis of quantization) as the molecule rotates, may be neglected as the rotational motion slows, could perhaps be carefully studied to yield conditions for approximately decoupling the allowed ESR transitions. This would greatly simplify the calculation of such cases in the very slow motional region.

Another possibility for the very slow motional region is based upon the analogy to the well-known exchange problem between different but discrete sites.[18] Thus, for example, in the two site case, when the jump rate between the two sites is slow compared to the spectral frequency difference associated with the sites, then one can decouple the rate equations and instead treat the resonance signal from each site independently but broadened by the uncertainty in lifetime broadening due to the jump process. In the present case of very slow tumbling there is a continuum of sites (i.e., orientations), so it is more difficult to develop a formal analogy (although computed results of the theory are consistent with such an analogy[19]). We have, in fact, studied in some detail the problem of using FE and of decoupling the elements by ignoring matching conditions between each element at the boundaries. This approach becomes rigorously sound in the rigid limit, but we find it breaks down even for very slow motions ($R/|\mathcal{F}| < 10^{-3}$) when Fourier series expansions are used to achieve convergence within each element. It is our belief that the possibility of decoupling each element, which could then be described by a small subset of local functions, still requires that an associated boundary-value problem be solved before the mathematical analogy with the jump problem between discrete sites might be realized. Problems of this sort are related to techniques in FE theory known as boundary solution procedures,[4] and it is our hope to study such approaches in an effort to simplify the analysis of spectra for slow tumbling.

[1] (a) J. H. Freed, G. V. Bruno, and C. F. Polnaszek, J. Phys. Chem. **75**, 3385 (1971); (b) G. V. Bruno, Ph.D. thesis, Cornell University, 1973.

[2] (a) J. H. Freed and J. B. Pedersen, Adv. Magn. Reson. **8**, 1 (1976); (b) J. Crank, *Mathematics of Diffusion* (Oxford University, London, 1975), 2nd ed.; (c) R. Richtmyer and K. Morton, *Difference Methods for Initial-Value Problems* (Wiley-Interscience, New York, 1967).

[3] G. P. Zientara and J. H. Freed, J. Chem. Phys. **70**, 2587 (1979).

[4] Engineering uses are discussed in O. Zienkiewicz, *The Finite Element Method* (McGraw-Hill, New York, 1977), 3rd ed., B. Finlayson, *The Method of Weighted Residuals and Variational Principles* (Academic, New York, 1972). Other chemical-physics applications are by A. Askar, J. Chem. Phys. **62**, 732 (1975) and by A. Askar, A. Cakmak, and H. Rabitz, Chem. Phys. **33**, 267 (1978).

[5] R. F. Campbell and J. H. Freed (to be published).

[6] J. H. Freed, in *Spin Labeling: Theory and Applications*, edited by L. Berliner (Academic, New York, 1976).

[7] R. Gordon and T. Messenger, in *Electron Spin Relaxation in Liquids*, edited by L. Muus (Plenum, New York, 1972); H. Silescu, J. Chem. Phys. **54**, 2110 (1971).

[8] T. J. Chung, *Finite Element Analysis in Fluid Dynamics* (McGraw-Hill, New York, 1978).

[9] See Footnote 12 of Ref. 3.

[10] An excellent presentation of Galerkin methods applied in the solution of parabolic equations is J. Douglas, Jr. and T. Dupont, SIAM J. Numer. Anal. **7**, 575 (1970).

[11] Although only spatial variables are used in this solution, we could have reformulated the numerical problem including ω (the Fourier transform or frequency variable) or s (the Laplace transform variable), or time as an additional independent variable. Here, though, we shall solve for the spatial and spin state distribution for a given value of ω.

[12] The functional exists for this simple problem [and can be derived from the information in Ref. 3, Eq. (2.19)]. Therefore we are implicitly satisfying a variational principle in this example, so our trial solution has the mathematical advantage of being a bound to the true solution. The use of integration by parts (or Gauss' theorem) creates a numerical problem similar, but not exactly the same, as one has in Ref. 3.

[13] Thus, discontinuous or rapidly oscillating functions (or their derivatives) cannot be properly included in a FD analysis without undue labor. However, they pose no drawback to an application of FE methods.

[14] One may also obtain a diagonal representation of ω by performing the average only on terms containing $\mathfrak{A}$, i.e., those terms with no angular dependence. We find, however, that better convergence is achieved if all the quantum terms are averaged.

[15] D. L. Williamson, J. Comp. Phys. **7**, 301 (1971).

[16] Analogous problems involving translational diffusion and spin-dependent phenomena have been discussed by Freed and Pedersen [Adv. Magn. Reson. **8**, 1 (1976)] and by Hwang and Freed [J. Chem. Phys. **63**, 4017 (1975)].

[17] E. Meirovitch and J. H. Freed (to be published).

[18] A. Abragam, *Principles of Nuclear Magnetism* (Oxford University, London, 1961).

[19] R. P. Mason and J. H. Freed, J. Phys. Chem. **78**, 1321 (1974).